IEEE Access
Multidisciplinary | Rapid Review | Open Access Journal

Received July 5, 2019, accepted July 21, 2019, date of publication July 24, 2019, date of current version August 12, 2019.

Digital Object Identifier 10.1109/ACCESS.2019.2930798

Integral Non-Singular Terminal Sliding Mode Controller for nth-Order Nonlinear Systems

REZA MOHAMMADI ASL[1], YASHAR SHABBOUEI HAGH[1], RAINER PALM[2], (Senior Member, IEEE), AND HEIKKI HANDROOS[1], (Member, IEEE)

[1]Laboratory of Intelligent Machines, Department of Mechanical Engineering, LUT University, FI-53850 Lappeenranta, Finland
[2]Centre for Applied Autonomous Sensor Systems (AASS), Örebro University, SE-70182 Örebr, Sweden

Corresponding author: Yashar Shabbouei Hagh (yashar.shabbouei.hagh@lut.fi)

ABSTRACT In this study, a new integral non-singular terminal sliding mode control method for nonlinear systems is introduced. The proposed controller is designed by defining a new sliding surface with an additional integral part. This new manifold is first introduced into the second-order system and then expanded to nth-order systems. The stability of the control system is demonstrated for both second-order and nth-order systems by using the Lyapunov stability theory. The proposed controller is applied to a robotic manipulator as a case study for second-order systems, and a servo-hydraulic system as a case study for third-order systems. The results are presented and discussed.

INDEX TERMS Integral non-singular terminal sliding mode controller, Lyapunov stability, robotic manipulator, servo-hydraulic system, trajectory tracking.

I. INTRODUCTION

In recent years, sliding mode control (SMC) has become one of the most intensive fields of research in the automatic control community because various advantages make this method suitable for different types of systems. Among the methods which tries to reduce final positioning errors due to input constraints, parametric uncertainties, and unmodeled dynamics by using different approaches such as neural networks or robust integral terms in the control law [1], [2], SMC is one of the well-known methods which has different advantages such as robust behavior in the presence of disturbances, finite time convergence and simple implementation. The main principle of the SMC method involves the use of a predetermined hyperplane called a sliding surface. SMC drags the nonlinear path to this sliding surface and after confining the system to this surface, the path slides along it to reach the origin. Different types of SMCs have been developed where they mainly differ in terms of their sliding surfaces [3]. The sliding surface selected for the basic versions of SMC is a linear surface. The main disadvantage of the basic method is the asymptotic stability problem, which cannot be considered a strong property for practical applications. Various studies have tried to address this disadvantage but it remains in the conventional sliding mode controllers [4]–[6].

The associate editor coordinating the review of this manuscript and approving it for publication was Ning Sun.

Among the different sliding methods developed to overcome this issue, the terminal SMC method guarantees finite time convergence when tracking the error to the origin [7]. This controller is designed by changing the sliding surface of the conventional SMC method in order to solve the stability problem. In addition, an adaptive global terminal SMC method was investigated by [8], where the proposed controller was developed to control uncertain nonlinear systems and guarantee the robustness property. However, this method is affected by a new problem because the singularity results in an unbounded control signal magnitude. Thus, new methods are required to solve this problem, such as the non-singular terminal sliding mode method [9], which has a wide range of application. For example, a non-singular terminal sliding mode method was employed to control a robotic manipulator [10]. This controller was applied to a system where the states were estimated using a nonlinear version of a Kalman filter and the performance of the controller was demonstrated in the presence of external disturbance. A new adaptive non-singular integral sliding mode controller was also proposed by [11] for controlling an autonomous underwater vehicle. It was demonstrated that the system could converge to the origin in finite time in the presence of uncertainties when the sliding surface was reached.

Various types of sliding mode controllers can be applied to different linear and nonlinear systems. Robotic systems and hydraulic systems are the two most common applications

of these control methods. Robotic systems comprise well-known second-order systems for testing the proficiency of controllers and various studies have investigated appropriate controllers for robotic systems [**?**], [**?**]. For instance, a PD controller was combined with a sliding mode controller for trajectory tracking in a robotic system [14], where this new control method aimed to exploit the advantages of both methods. In addition, a hydraulic system can be selected as an appropriate testbed for various reasons. First, this type of system exhibits third-order dynamics, which is challenging for the controller. Second, different types of model uncertainties make it difficult to stabilize the system. Thus, several types of controllers have been introduced for these systems. In particular, a new disturbance rejection method was employed and implemented based on a hydraulic system by [15]. Several versions of SMC approaches have been applied to robotic and hydraulic systems [16], [17]. An integral SMC method was developed by [18] for a robotic system, which made the tracking error tend to zero in finite time while also eliminating the chattering problem phenomenon. A discrete time SMC approach was developed for a hydraulic system by [19] and applied to a hydraulic system, where it obtained appropriate behavior without involving a switching-type reaching law. The main drawbacks of these previously proposed methods can be summarized as follows.

- System diversity: most previously proposed methods are suitable only for second-order systems. The development of these methods for higher order systems was not discussed or it was too complex to implement.
- Excessive amounts of tunable parameters: several methods combined an SMC method with other types of traditional methods such as PD or PID controllers, thereby leading to new problems because many parameters must be tuned when optimizing the controller,
- Singularity: some of the previously introduced versions of SMC lead to an unbounded control signal magnitude known as singularity, which is an unsolved problem according to reviews.

In order to address the need for new methods to solve the problems of previously proposed methods, a new nonlinear sliding surface method is introduced called an integral non-singular terminal sliding mode controller (INTSMC). The main contributions of this study are as follows.

- Sliding surface: a new integral part is added to the sliding surface of the controller, which improves the robustness of the controller
- System diversity: the controller is designed for second-order and nth-order systems, which makes the controller suitable for various practical systems
- Singularity problem: different conditions are considered in the design procedure to solve the singularity problem.

The proposed controller is tested with two types of systems: a robotic manipulator and a servo-hydraulic system. The former system was considered as a case study of second-order systems and the latter as a case study of third-order systems.

The remainder of this paper is organized are follows. Section II describes the controller designed for second- and nth-order systems as well as presenting the stability analysis. Section III presents the simulation results obtained for the controller of a robotic system as a study case of second-order systems, and for a hydraulic system as a study case of third-order systems. Finally, conclusions are given in Section IV.

II. INTSMC

In this section, a new version of SMC with a nonlinear sliding surface is presented. In order to validate the effectiveness of this controller, INTSMC strategies are proposed for second- and nth-order systems in the following.

A. INTSMC FOR SECOND-ORDER SYSTEMS

Consider a second-order nonlinear system:

$$\begin{aligned} \dot{x}_1 &= x_2 \\ \dot{x}_2 &= f(x) + b(x)u + d(x), \end{aligned} \tag{1}$$

where the system states are represented by $x = [x_1 \;\; x_2]^T \in R^n$ vector, $f(x)$ and $b(x) \neq 0$ are nonlinear functions, and $d(x)$ indicates the disturbance and uncertainties, which satisfy $\| d(x) \| \leqslant \zeta_d$, where $\zeta_d > 0$ has a constant value.

Consider a twice differentiable desired trajectory, $x_d(t) \in R^n$, with respect to time. In terms of the definitions of the tracking error vector and its derivative given as $e = x_1 - x_{1d}$, $\dot{e} = \dot{x_1} - \dot{x}_{1d}$, respectively, as well as the model given in Eq.(1), the error dynamics can be written as:

$$\ddot{e} = f(x) + b(x)u + d(x) - \ddot{x}_{1d}. \tag{2}$$

For the error vectors given above, the sliding surface can be written as:

$$s = e + \int_0^t \left(c_1 \mathrm{sgn}(\dot{e}) |\dot{e}|^{\alpha_1} + c_2 \mathrm{sgn}(e) |e|^{\alpha_2} \right) dt, \tag{3}$$

where c_1 and c_2 are positive constants. It is also supposed that $1 < \alpha_1 < 2$ and $\alpha_2 = \alpha_1/(2 - \alpha_1)$. To guarantee the convergence of s to zero in finite time and to eliminate the chattering problem, the following INTSMC surface is proposed:

$$\begin{aligned} \sigma &= \dot{s} + \lambda s \\ &= \dot{e} + c_1 \mathrm{sgn}(\dot{e}) |\dot{e}|^{\alpha_1} + c_2 \mathrm{sgn}(e) |e|^{\alpha_2} + \ldots \\ &\quad \lambda \left(e + \int_0^t \left(c_1 \mathrm{sgn}(\dot{e}) |\dot{e}|^{\alpha_1} + c_2 \mathrm{sgn}(e) |e|^{\alpha_2} \right) dt \right), \end{aligned} \tag{4}$$

where λ is a positive tuning constant.

For the system given in (1) with the sliding variable in Eq.(3), the controller can be obtained as follows.

$$\begin{aligned} \dot{\sigma} &= \ddot{s} + \lambda \dot{s} \\ &= \left(\ddot{e} + c_1 \alpha_1 \ddot{e} |\dot{e}|^{\alpha_1 - 1} + c_2 \alpha_2 \dot{e} |e|^{\alpha_2 - 1} \right) + \ldots \\ &\quad \lambda \left(\dot{e} + c_1 \mathrm{sgn}(\dot{e}) |\dot{e}|^{\alpha_1} + c_2 \mathrm{sgn}(e) |e|^{\alpha_2} \right) \end{aligned}$$

$$\xrightarrow{Eq.(2)} = \Big[f(x)+b(x)u+d(x)-\ddot{x}_d+c_2\alpha_2\dot{e}|e|^{\alpha_2-1}\ldots$$
$$c_1\alpha_1\left(f(x)+b(x)u+d(x)-\ddot{x}_d\right)|\dot{e}|^{\alpha_1-1}\Big]+\ldots$$
$$\lambda\left(\dot{e}+c_1\mathrm{sgn}(\dot{e})|\dot{e}|^{\alpha_1}+c_2\mathrm{sgn}(e)|e|^{\alpha_2}\right)$$
$$\xrightarrow{\dot{\sigma}=0} u = -b^{-1}(x)\Big[-\ddot{x}_d+f(x)+\frac{\lambda}{1+c_1\alpha_1|\dot{e}|^{\alpha_1-1}}$$
$$\times\left(\dot{e}+c_1\mathrm{sgn}(\dot{e})|\dot{e}|^{\alpha_1}+c_2\mathrm{sgn}(e)|e|^{\alpha_2}\right)+\ldots$$
$$\frac{1}{1+c_1\alpha_1|\dot{e}|^{\alpha_1-1}}\left(c_2\alpha_2\dot{e}|e|^{\alpha_2-1}\right)\Big]-\ldots$$
$$b^{-1}(x)\left\{(\zeta_d+\eta)\,\mathrm{sgn}(\sigma)\right\} \quad (5)$$

The controller comprises an equivalent control part, u_{eq}, and a switching control part, u_{sw}, which is defined as follows.

$$u_{eq} = -b^{-1}(x)\Big[-\ddot{x}_d+f(x)+\frac{\lambda}{1+c_1\alpha_1|\dot{e}|^{\alpha_1-1}}$$
$$\times\left(\dot{e}+c_1\mathrm{sgn}(\dot{e})|\dot{e}|^{\alpha_1}+c_2\mathrm{sgn}(e)|e|^{\alpha_2}\right)+\ldots$$
$$\frac{1}{1+c_1\alpha_1|\dot{e}|^{\alpha_1-1}}\left(c_2\alpha_2\dot{e}|e|^{\alpha_2-1}\right)\Big]$$
$$u_{sw} = -b^{-1}(x)\left(\zeta_d+\eta\right)\mathrm{sgn}(\sigma) \quad (6)$$

Theorem 1: The origin of the second-order system given in Eq.(1) *converges to zero in finite time by using the controlling law given in Eq.*(5).

Proof: Consider the Lyapunov function $V = 1/2\sigma^2$ that should satisfy $\dot{V} = 1/2\frac{d}{dt}\sigma^2 \leq -\eta|\sigma|$ in which $\eta > 0$:

$$\sigma\dot{\sigma} = \sigma\Big[\left(\ddot{e}+c_1\alpha_1\ddot{e}|\dot{e}|^{\alpha_1-1}+c_2\alpha_2\dot{e}|e|^{\alpha_2-1}\right)+\ldots$$
$$\lambda\left(\dot{e}+c_1\mathrm{sgn}(\dot{e})|\dot{e}|^{\alpha_1}+c_2\mathrm{sgn}(e)|e|^{\alpha_2}\right)\Big]$$
$$\xrightarrow{Eq.(2)} = \sigma\Big[\Big(f(x)+b(x)u+d(x)-\ddot{x}_d+\ldots$$
$$c_1\alpha_1\left(f(x)+b(x)u+d(x)-\ddot{x}_d\right)|\dot{e}|^{\alpha_1-1}+\ldots$$
$$c_2\alpha_2\dot{e}|e|^{\alpha_2-1}\Big)\Big]+\ldots$$
$$\sigma\left[\lambda\left(\dot{e}+c_1\mathrm{sgn}(\dot{e})|\dot{e}|^{\alpha_1}+c_2\mathrm{sgn}(e)|e|^{\alpha_2}\right)\right]$$
$$\xrightarrow{Eq.(5)} = \sigma\left\{\left(1+c_1\alpha_1|\dot{e}|^{\alpha_1-1}\right)\left(d(x)-(\zeta_d+\eta)\mathrm{sgn}(\sigma)\right)\right\}, \quad (7)$$

which is:

$$\dot{V} \leqslant -\Pi\mid\sigma\mid<0, \quad (8)$$

where

$$\xrightarrow[1<\alpha_1<2]{\eta>0} \Pi = \left(1+c_1\alpha_1|\dot{e}|^{\alpha_1-1}\right)\eta > 0. \quad (9)$$

Therefore, based on the Lyapunov stability criteria, the integral non-singular terminal sliding mode (INTSM) surface in (4) converges to zero in finite time. This completes the proof. ■

B. INTSMC FOR NTH -ORDER SYSTEMS

Consider an nth-order nonlinear system:

$$\begin{aligned}\dot{x}_1 &= x_2\\ \dot{x}_2 &= x_3\\ &\vdots\\ \dot{x}_n &= f(x)+b(x)u+d(x),\end{aligned} \quad (10)$$

where the system states are represented by $x = [x_1, x_2, \ldots, x_n]^T \in R^n$ vector, and $f(x)$, $b(x) \neq 0$, and $d(x)$ are the same as those given in Eq.(1). By defining the tracking error vectors and their derivatives, the error dynamics can be written as follows.

$$\begin{aligned}e &= x_1 - x_{1d}\\ \dot{e} &= \dot{x_1} - \dot{x}_{1d}\\ &\vdots\\ e^{(n)} &= f(x)+b(x)u+d(x)-x_{1d}^{(n)}\end{aligned} \quad (11)$$

An INTSM manifold is selected for system (10) as follows:

$$s = e+\int_0^t\left(\sum_{i=1}^{n}c_i\mathrm{sgn}(e^{(n-i)})|e^{(n-i)}|^{\alpha_i}\right)dt, \quad (12)$$

where c_i are positive constants, which are selected such that the real polynomial $p, p(r) = r^n + c_1 r^{n-1} + \cdots + c_{n-1}r + c_n$, $r \in \mathbb{R}$ satisfies Hurwitz stability criteria, and $1 < \alpha_i < 2$ for $i = 1, \alpha_i = \alpha_{i-1}/(2-\alpha_{i-1})$ for $i = 2, \ldots, n$.

Given the following surface:

$$\sigma = \dot{s}+\lambda s$$
$$= \dot{e}+\sum_{i=1}^{n}c_i\mathrm{sgn}(e^{(n-i)})|e^{(n-i)}|^{\alpha_i}+\ldots$$
$$\lambda\left(e+\int_0^t\left(\sum_{i=1}^{n}c_i\mathrm{sgn}(e^{(n-i)})|e^{(n-i)}|^{\alpha_i}\right)dt\right), \quad (13)$$

the convergence of s to zero in finite time is satisfied, where λ is a positive tuning constant.

For the system given in Eq.(10) and the sliding surface in (13), the controller can be obtained as follows.

$$\dot{\sigma} = \ddot{s}+\lambda\dot{s}$$
$$= \ddot{e}+\sum_{i=1}^{n}\alpha_i c_i|e^{(n-i)}|^{\alpha_i-1}e^{(n-i+1)}+\ldots$$
$$\lambda\left(\dot{e}+\sum_{i=1}^{n}c_i\mathrm{sgn}(e^{(n-i)})|e^{(n-i)}|^{\alpha_i}\right)$$
$$= \ddot{e}+\lambda\left(\dot{e}+\sum_{i=1}^{n}c_i\mathrm{sgn}(e^{(n-i)})|e^{(n-i)}|^{\alpha_i}\right)+\ldots$$
$$\sum_{i=2}^{n}\alpha_i c_i|e^{(n-i)}|^{\alpha_i-1}e^{(n-i+1)}+\ldots$$
$$\alpha_1 c_1|e^{(n-1)}|^{\alpha_1-1}e^{(n)}$$

$$\xrightarrow{Eq.(11)} = \ddot{e} + \lambda\left(\dot{e} + \sum_{i=1}^{n} c_i \text{sgn}(e^{(n-i)})|e^{(n-i)}|^{\alpha_i}\right) + \ldots$$
$$\sum_{i=2}^{n} \alpha_i c_i |e^{(n-i)}|^{\alpha_i - 1} e^{(n-i+1)} + \ldots$$
$$\alpha_1 c_1 |e^{(n-1)}|^{\alpha_1 - 1}\left(f(x) + b(x)u + d(x) - x_{1d}^{(n)}\right)$$
$$\xrightarrow{\dot{\sigma}=0} u = -b^{-1}(x)\Bigg[f(x) - x_{1d}^{(n)} + \frac{1}{c_1\alpha_1}|e^{(n-1)}|^{1-\alpha_1}\Bigg[\ddot{e} + \ldots$$
$$\lambda\left(\dot{e} + \sum_{i=1}^{n} c_i \text{sgn}(e^{(n-i)})|e^{(n-i)}|^{\alpha_i}\right) + \ldots$$
$$\sum_{i=2}^{n} \alpha_i c_i |e^{(n-i)}|^{\alpha_i - 1} e^{(n-i+1)}\Bigg] + (\zeta_d + \eta)\text{sgn}(\sigma)\Bigg] \tag{14}$$

Theorem 2: The origin of the nth-order system given in Eq.(10) *converges to zero in finite time by using the controlling law in Eq.*(14).

Proof: Consider the Lyapunov function $V = 1/2\sigma^2$ that should satisfy $\dot{V} = 1/2\frac{d}{dt}\sigma^2 \leq -\eta|\sigma|$ in which $\eta > 0$:

$$\dot{V} = \sigma\dot{\sigma}$$
$$= \sigma\Bigg[\alpha_1 c_1 |e^{(n-1)}|^{\alpha_1 - 1}\left(f(x) + b(x)u + d(x) - x_{1d}^{(n)}\right)$$
$$+ \ddot{e} + \lambda\left(\dot{e} + \sum_{i=1}^{n} c_i \text{sgn}(e^{(n-i)})|e^{(n-i)}|^{\alpha_i}\right) + \ldots$$
$$\sum_{i=2}^{n} \alpha_i c_i |e^{(n-i)}|^{\alpha_i - 1} e^{(n-i+1)}\Bigg]$$
$$\xrightarrow[Eq.(11)]{Eq.(14)} = \sigma\left\{\alpha_1 c_1 |e^{(n-1)}|^{\alpha_1 - 1}\left(d(x) - (\zeta_d + \eta)\text{sgn}(\sigma)\right)\right\}$$
$$\Longrightarrow \dot{V} \leqslant -\alpha_1 c_1 |e^{(n-1)}|^{\alpha_1 - 1}\eta \mid \sigma \mid, \tag{15}$$

and since $\eta\alpha_1 c_1 |e^{(n-1)}|^{\alpha_1 - 1} > 0$, then based on the Lyapunov stability criteria, the INTSM surface in (13) converges to zero in finite time. This completes the proof. ■

This should be noted that the sign function used in the switching part of the control low can cause a chattering phenomenon. To have a chattering-free control signal, this discontinuous sign function is replaced with a continuous hyperbolic tangent function.

III. SIMULATION RESULTS

In the following, the results obtained from studies of a two degrees of freedom (2-DoF) robot manipulator and an application to a servo-hydraulic system are presented. In order to evaluate the effectiveness of the proposed INTSM controller, a simulation was conducted of a 2-DoF robot as an example of a second-order system. The capacity of the controller was also investigated based on a servo-hydraulic system as an example of a third-order system model.

A. 2-DOF ROBOT MANIPULATOR

In order to test the performance of the proposed controller in second-order systems, it was applied to a robotic manipulator as a well-known example of a second-order system. A two-link rigid manipulator was selected for this simulation. A general schematic of the two-link rigid robot is shown in Fig. 1

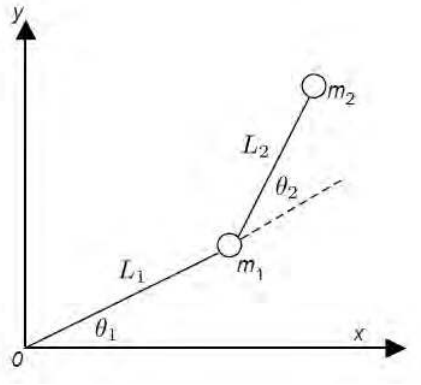

FIGURE 1. 2-DoF robot manipulator model.

TABLE 1. Values of the parameters in Fig.1.

Link	mass (kg)	Length (m)
First link	$m_1 = 0.5$	$L_1 = 1.0$
Second link	$m_2 = 0.8$	$L_2 = 0.8$

The dynamic equations for the rigid manipulator can be written as:

$$D(\theta)\ddot{\theta} + C(\theta, \dot{\theta})\dot{\theta} + g(\theta) = \tau, \tag{16}$$

where $D(\theta) \in R^{n\times n}$ is the inertia matrix, $C(\theta, \dot{\theta})\dot{\theta} \in R^n$ are centripetal and Coriolis forces, $g(\theta) \in R^n$ is the gravitational force, and τ is the exerted joint input. The dynamic equation of the robot is given in Eq.(17) where the abbreviations $s_i = sin(\theta_i)$ and $c_i = cos(\theta_i)$ are used. The parameters used in Eq.(17) are shown in Table 1.

$$\begin{bmatrix} (m_1 + m_2)L_1^2 + m_2L_2^2 + 2m_2L_1L_2cos(\theta_2) & m_2L_2^2 + m_2L_1L_2cos(\theta_2) \\ m_2L_2^2 + m_2L_1L_2cos(\theta_2) & m_2L_2^2 \end{bmatrix}\begin{bmatrix}\ddot{\theta}_1 \\ \ddot{\theta}_2\end{bmatrix}$$
$$+ \begin{bmatrix} -m_2L_1L_2sin(\theta_2)\dot{\theta_1}^2 - 2m_2L_1L_2sin(\theta_2)\dot{\theta}_1\dot{\theta}_2 \\ m_2L_1L_2sin(\theta_2)\dot{\theta_2}^2 \end{bmatrix}$$
$$+ \begin{bmatrix} ((m_1 + m_2)L_1cos(\theta_2) + m_2L_2cos(\theta_1 + \theta_2))\, g \\ (m_2L_2cos(\theta_1 + \theta_2))\, g \end{bmatrix} = \begin{bmatrix}\tau_1 \\ \tau_2\end{bmatrix} \tag{17}$$

where $g = 9.81(kgm/s^2)$. In order to have a feasible model as Eq. (1), the state space representation of robot manipulator can be obtained as, $f = -D(\theta)^{-1}\left(C\left(\theta, \dot{\theta}\right)\dot{\theta} + g(\theta)\right)$, and $b = D(\theta)^{-1}$.

The initial state conditions were set to $x_0 = [\theta_1 \quad \theta_2 \quad \dot{\theta}_1 \quad \dot{\theta}_2] = [1(rad), \quad 1.5(rad), \quad 0(rad/s), \quad 0(rad/s)]^T$ and the desired trajectories are as follows.

$$\theta_{d_1} = -pi/2 + 0.92 \cdot (1 - cos(1.26 - t/2))$$
$$\theta_{d_2} = -pi/5 + 0.92 \cdot (1 - cos(1.26 - t)) \tag{18}$$

TABLE 2. Parameter values used in the INTSMC for the robot manipulator.

Parameters	c_1	c_2	α_1	λ	$\zeta_d + \eta$
Values	0.1	0.1	1.0010	10	50

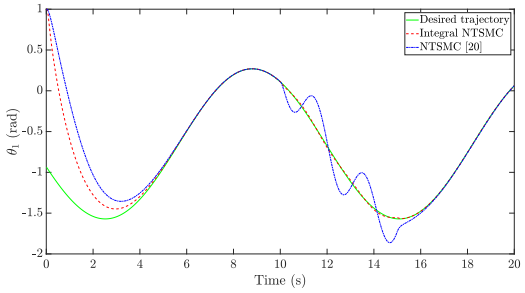

(a) Values of θ_1

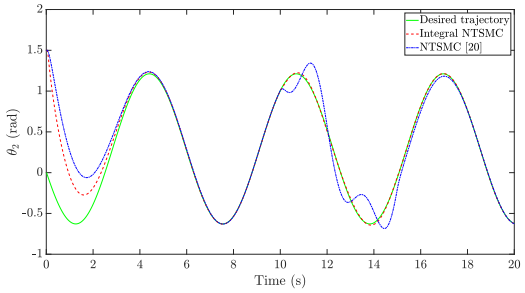

(b) Values of θ_2

FIGURE 2. 2-DoF performance based on proposed INTSMC in comparison to NTSMC [20].

The tuning parameters, which are selected based on the designers experience, are shown in Table 2 for the INTSM manifold in Eq.(3). It should be noted that in cases that the real system might face an external disturbance, the designers choose the upper bound based on previous experiments. In order to compare the proposed controller with other previously proposed controllers, the non-singular terminal sliding mode (NTSM) controller proposed by [20] is considered. In the sliding manifold proposed by [20], $s = e + \frac{1}{\beta}\dot{e}^{p/q}$, where p and q are selected such that $1 < p/q < 2$. It also assumed that from $t = 10s$ to $t = 15s$, the external disturbance of $d(x) = 10sin(3t)$ affects the robot. Using the same values for $1/\beta = c_1$ and $p/q = \alpha_3$, the INTSMC and non-singular terminal sliding mode controller (NTSMC) are compared in Fig.2, which indicates that the desired reference signals were tracked correctly after a transient phase of $4 - 5$ s. However, within the time period when an external disturbance affected the system, the proposed INTSMC was more capable of handling the disturbance than the NTSMC, as shown clearly by the tracking error for each link using INTSMC and NTSMC in Fig.3. Thus, the proposed INTSMC performed better rather than the NTSMC. The root mean square error (RMSE) for each link is calculated to demonstrate the superior performance of the INTSMC compared with the conventional NTSMC, as shown in Table 3,

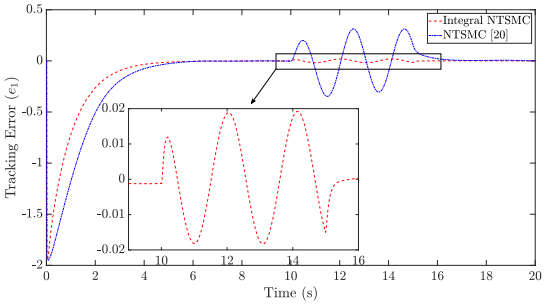

(a) Values of $e(\theta_1)$

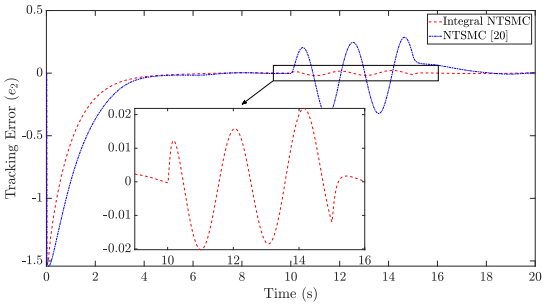

(b) Values of $e(\theta_2)$

FIGURE 3. Reference signals tracking error based on INTSMC and NTSMC [20] for the robot manipulator.

TABLE 3. Root mean square errors calculated for the proposed INTSMC and NTSMC [20].

Controller	First link	Second link
Integral NTSMC	0.0004	0.0019
NTSMC [20]	0.0090	0.0260

The sliding surface and the control signal for the proposed INTSMC are shown in Fig. 4 and Fig. 5, respectively. The reason for a high value of control signal at the beginning is due to the attempt that the controller made to have faster convergence rate. The changes in the control signals during $t = 10 - 15s$ are clearly visible in these figures, but the conventional NTSMC was not capable of tracking the desired path correctly even with this change.

B. HYDRAULIC SYSTEM

The application of the proposed controller to a higher order system is considered to validate the proposed approach. A servo-hydraulic system is selected as an example of a third-order system for validating and testing the proposed controller. A schematic of the selected servo-hydraulic system is shown in Fig. 6. In the following, the model of the servo-hydraulic system and the simulation results are presented.

Newton's equation is applied to the mass to model the cylinder part, so the movement equation can be written as:

$$M\ddot{x}_P = -b\dot{x}_P + A_1 p_1 - A_2 p_2 - F_e, \tag{19}$$

where x_P denotes the piston position. The pressure and area of the cylinder are represented by $p_{1,2}$ and $A_{1,2}$, respectively.

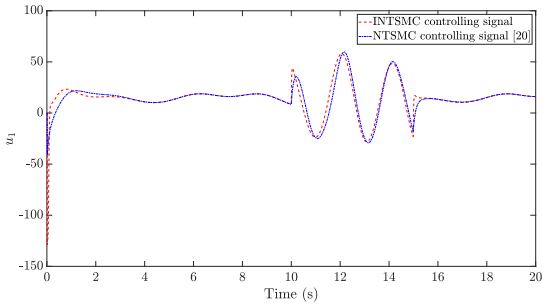

(a) Values of u_1

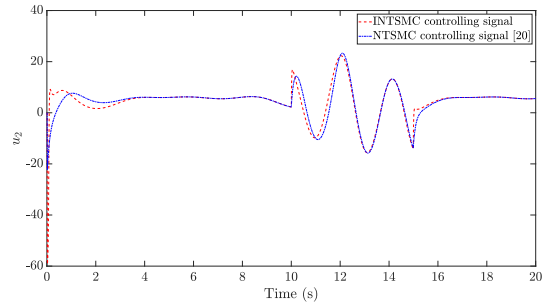

(b) Values of u_2

FIGURE 4. Control signals of INTSMC and NTSMC [20] for the robot manipulator.

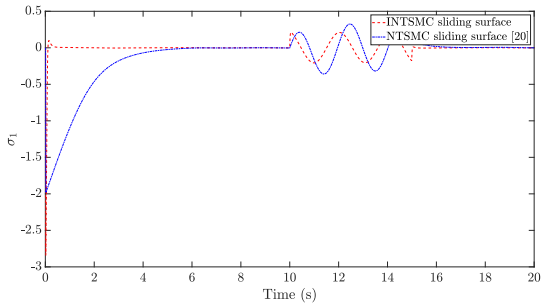

(a) Values of σ_1

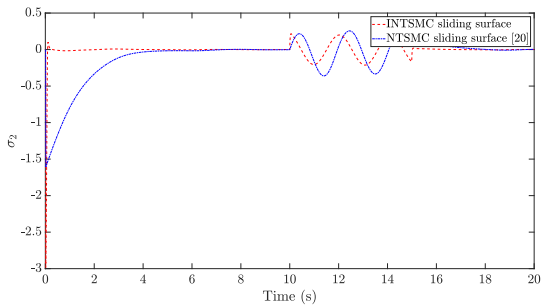

(b) Values of σ_2

FIGURE 5. Sliding surfaces of INTSMC and NTSMC [20] for the robot manipulator.

The parameters M, F_e, and b represent the load mass, external force, and friction, respectively [21]. In (19), in order to calculate the position x_P of the piston, it is necessary to determine values of the pressures $p_{1,2}$ on the two sides of the cylinder. By applying basic hydraulic rules [22], the pressures

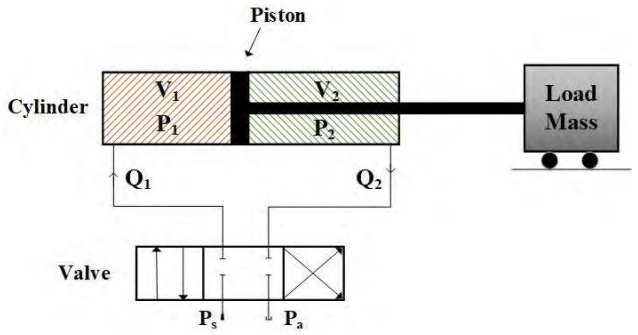

FIGURE 6. The schematic of servo-hydraulic system.

TABLE 4. Parameter values used in the INTSMC for the servo-hydraulic system.

Parameters	c_1	c_2	c_3	α_1	λ	$\zeta_d + \eta$
Values	2.1	4.7	1.5	1.0010	3	10

on the two sides of the cylinder can be obtained using the following equations:

$$\begin{aligned} \dot{P}_1 &= \frac{\beta_e}{V_1}\left(Q_1 - A_1\dot{x}_P + Q_I - Q_{E1}\right) \\ \dot{P}_2 &= \frac{\beta_e}{V_2}\left(Q_2 - A_2\dot{x}_P - Q_I - Q_{E2}\right), \end{aligned} \tag{20}$$

where the flows on each side of the cylinder are represented by Q_1 and Q_2. The parameters β_e, V_1, and V_2 represent the bulk modulus and the volumes of each side of the cylinder, respectively. The internal leakage and the external leakage on each side are given by Q_I, Q_{E1}, and Q_{E2}, respectively. The different flows in the hydraulic circuit can be formulated as:

$$\begin{aligned} Q_1 &= \begin{cases} C_s u\sqrt{p_s - p_1} & u \geq 0 \\ C_s u\sqrt{p_1 - p_a} & u < 0 \end{cases} \\ Q_2 &= \begin{cases} C_s u\sqrt{p_2 - p_a} & u \geq 0 \\ C_s u\sqrt{p_s - p_2} & u < 0 \end{cases} \\ Q_I &= K_i\left(p_2 - p_1\right), \\ Q_{E1} &= K_{E1}\left(p_1 - p_a\right), \\ Q_{E2} &= K_{E2}\left(p_2 - p_a\right), \end{aligned} \tag{21}$$

where C_s represents the flow coefficient. The internal and external leakage flow coefficients for each side of cylinder are given by K_i, K_{E1}, and K_{E2}, respectively. In Eq. (20), it is necessary to determine the volumes V_1 and V_2 on the different sides of the cylinder, which are calculated as:

$$\begin{aligned} V_1 &= A_1 x_P + v_{01} \\ V_2 &= A_2\left(L - x_P\right) + v_{02}, \end{aligned} \tag{22}$$

where the pipeline volumes for each side of the cylinder are given by $v_{0i}, i = 1, 2$ [23]. The parameter L represents the maximum value of the piston position. In order to apply SMC, the proposed model of the system should be defined as a model with Eq. (10). According to Eqs. (19)–(21),

TABLE 5. Parameter values for the servo-hydraulic system in SI units.

Parameters	Values	Parameters	Values
M	270	b	418.33
A_1	8.04×10^{-4}	A_2	4.24×10^{-4}
v_{01}	2.13×10^{-4}	v_{02}	1.07×10^{-4}
P_s	14	P_a	0.9
L	1	β_e	7×10^8

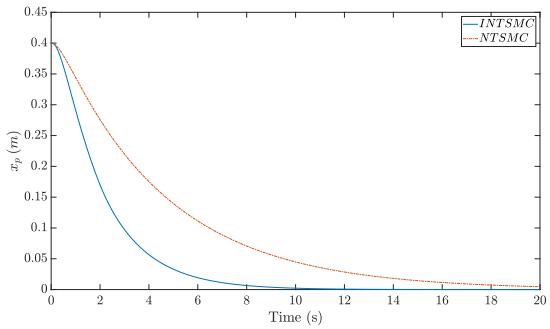

(a) Values of x_P

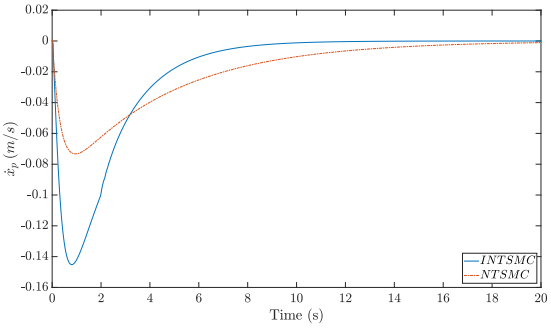

(b) Values of $\dot{x}_P$

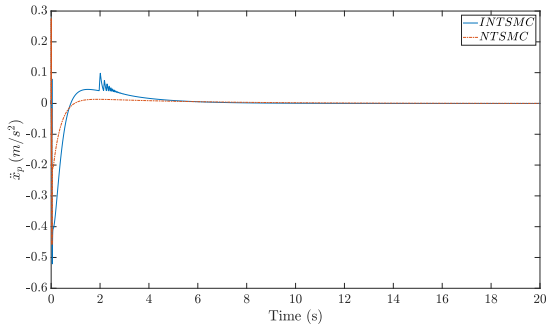

(c) Values of $\ddot{x}_P$

FIGURE 7. The comparison of INTSMC and NTSMC [20] for values of the states of the controlled system.

the hydraulic model is not appropriate for the application of the proposed sliding mode controller. Thus, in order to obtain a feasible model of the designed controller, the derivative of the movement equation of the piston position is taken and it is concluded:

$$\begin{aligned}\frac{d}{dt}\left(M\ddot{x}_P\right) &= \frac{d}{dt}\left(-b\dot{x}_P + A_1 p_1 - A_2 p_2 - F_e\right)\\ &= -b\ddot{x}_P + A_1\dot{p}_1 - A_2\dot{p}_2 - \dot{F}_e. \end{aligned} \tag{23}$$

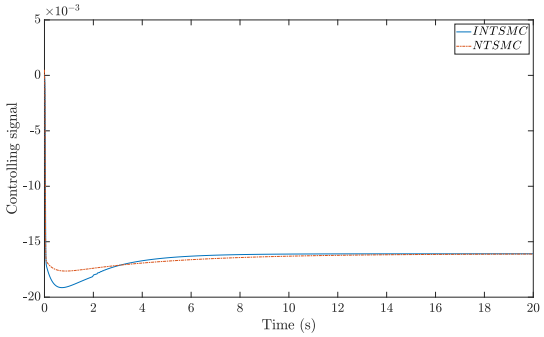

FIGURE 8. The comparison of the control signal of INTSMC and NTSMC [20].

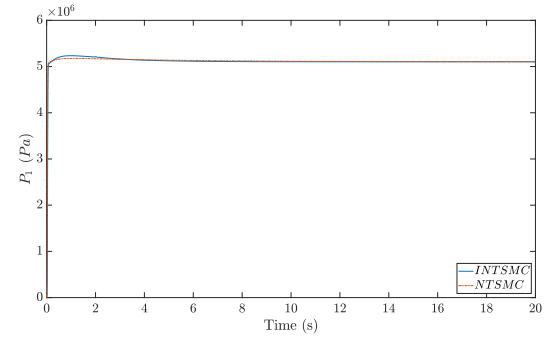

(a) Values of P_1

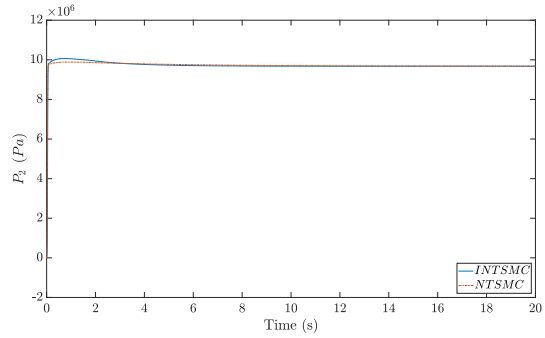

(b) Values of P_2

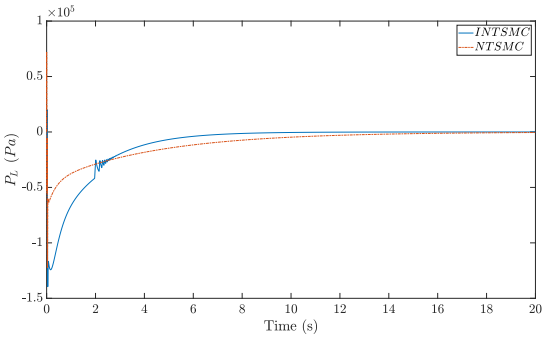

(c) Values of P_L

FIGURE 9. The pressure values of the hydraulic circuit.

Now, a new parameter is defined as $P_L = p_1 - \frac{A_2}{A_1}p_2$, which is the load pressure. In previous studies [24], [25], the load flow was defined as $Q_L = \frac{Q_1+Q_2}{2}$, which can be expressed as

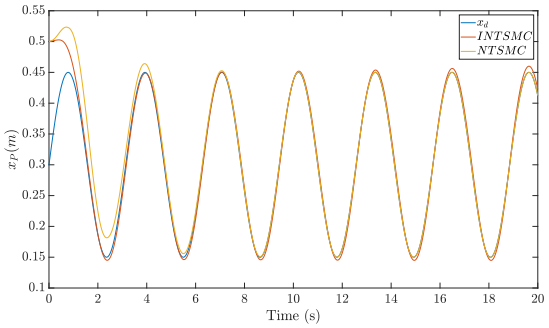

(a) Values of x_P

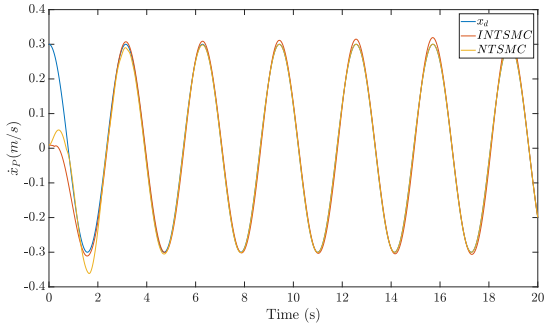

(b) Values of $\dot{x}_P$

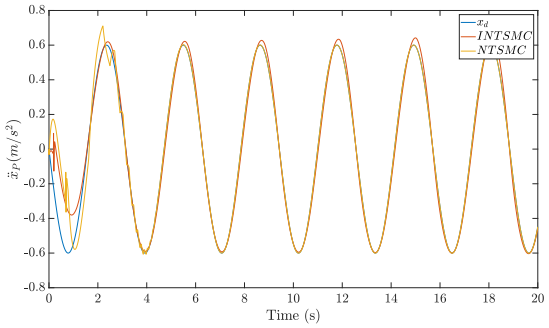

(c) Values of $\ddot{x}_P$

FIGURE 10. The comparison of INTSMC and NTSMC [20] for values of states of the controlled servo-hydraulic system.

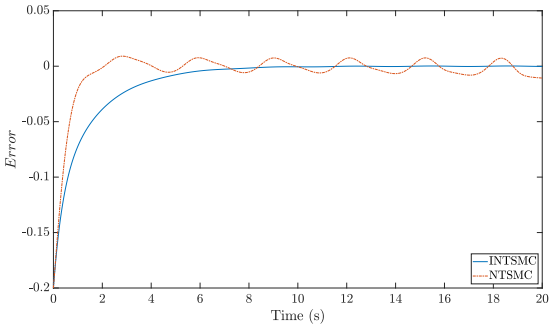

(a) Values of $E[x_P]$

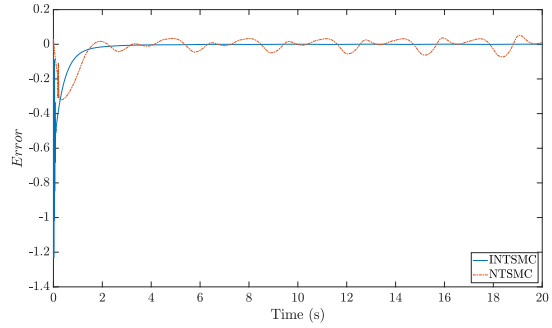

(b) Values of $E[\dot{x}_P]$

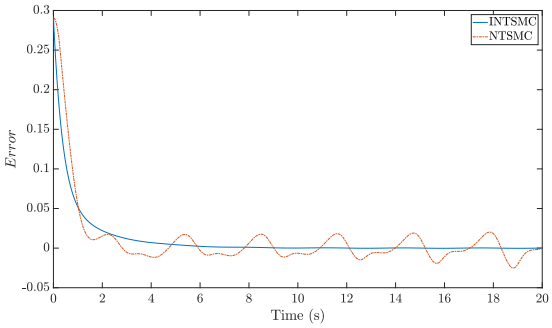

(c) Values of $E[\ddot{x}_P]$

FIGURE 11. The comparison of tracking error of INTSMC and NTSMC [20] for states of the controlled servo-hydraulic system.

follows.

$$Q_L = \begin{cases} \frac{C_s x_P}{2}\left(\sqrt{p_s - p_1} + \sqrt{p_2 - p_a}\right) & u \geq 0 \\ \frac{C_s x_P}{2}\left(\sqrt{p_1 - p_a} + \sqrt{p_s - p_2}\right) & u < 0 \end{cases} \tag{24}$$

Given the new definitions and the equations above, the servo-hydraulic system can be defined as a function of three variables $(x_P, \dot{x}_P, P_L)$:

$$M\dddot{x}_P = -b\ddot{x}_P + A_1\dot{P}_L - \dot{F}_e. \tag{25}$$

According to Eq. (25), the state space of the system can be represented as follows:

$$\begin{aligned} \dot{x}_1 &= x_2 \\ \dot{x}_2 &= x_3 \\ \dot{x}_3 &= \frac{1}{M}\left(-bx_2 + A_1\dot{P}_L - \dot{F}_e\right), \end{aligned} \tag{26}$$

where the new state variables are defined as $X = [x_1, x_2, x_3]^T = [x_P, \dot{x}_P, \ddot{x}_P]^T$. By using the definition of the load pressure and substituting the values for the different sides of cylinder from Eq. (20) into the equation for the third state of the hydraulic system (Eq. (26)), it can be obtained:

$$\dot{x}_3 = \frac{1}{M}\left(-bx_2 + \varphi(P_L)u + \psi(P_L) - \dot{F}_e\right), \tag{27}$$

where the functions $\varphi(.)$, and $\psi(.)$ are nonlinear functions that denote the uncertainties in the model. The final state space model for the servo-hydraulic system used by the proposed controller can be expressed as follows.

$$\begin{aligned} \dot{x}_1 &= x_2 \\ \dot{x}_2 &= x_3 \\ \dot{x}_3 &= \frac{1}{M}\left(-bx_2 + \varphi(P_L)u + \psi(P_L) - \dot{F}_e\right) \end{aligned} \tag{28}$$

TABLE 6. Root mean square errors with the proposed INTSMC and NTSMC [20] when tracking the error based on a servo-hydraulic system.

Controllers	x_p	$\dot{x}_p$	$\ddot{x}_p$
Integral NTSMC	0.0236	0.0334	0.0528
NTSMC [20]	0.1312	0.1452	0.1637

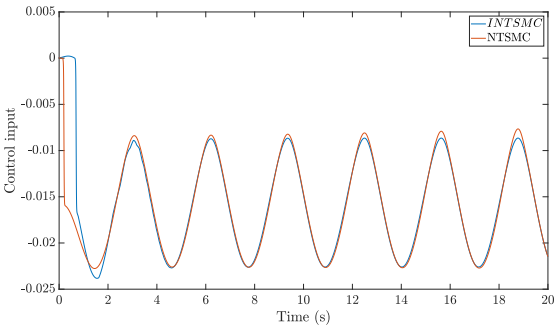

(a) Control signal

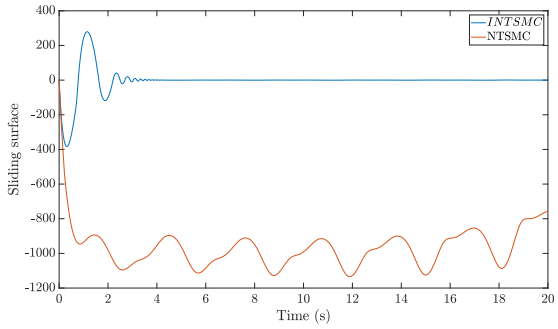

(b) Sliding surface

FIGURE 12. The comparison of the control signal and the sliding surface of INTSMC and NTSMC [20] for tracking a desired path.

The results obtained after applying the proposed controller to this model are presented in the following. Two scenarios are considered for the simulation: reaching the origin and tracking a desired path. For both scenarios, the parameters of the controller are set as Table 4. Simulation results are obtained with the proposed controller based on the servo-hydraulic system defined by Eq.(28). The parameters used in the simulation are given in Table 5 [21]. In order to demonstrate the performance and robustness of the designed approach with a third-order system, the simulation was conducted in the presence of uncertainties in the servo-hydraulic system, which were modeled in terms of the load mass. This assumption can be formulated as follows:

$$\begin{aligned}\dot{x}_1 &= x_2\\ \dot{x}_2 &= x_3\\ \dot{x}_3 &= \frac{1}{M+\delta}\left(-bx_2+\varphi(P_L)u+\psi(P_L)-\dot{F}_e\right),\end{aligned} \quad (29)$$

where δ is the uncertainty in the model, which can be bounded as $0 \leq \delta \leq 60$. According to these definitions and the uncertainties in the system model, the proposed method was applied to the system. The initial values for the starting points were $X_0 = [x_{10}, x_{20}, x_{30}]^T = [0.4, 0.005, 0]^T$. The results

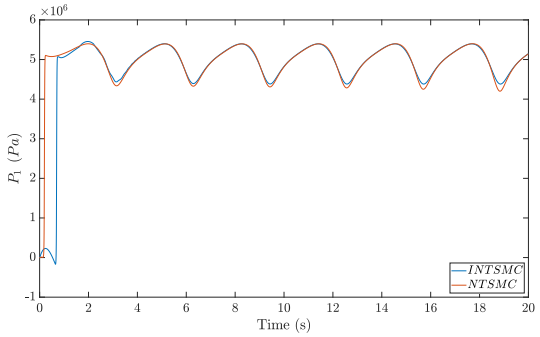

(a) Values of P_1

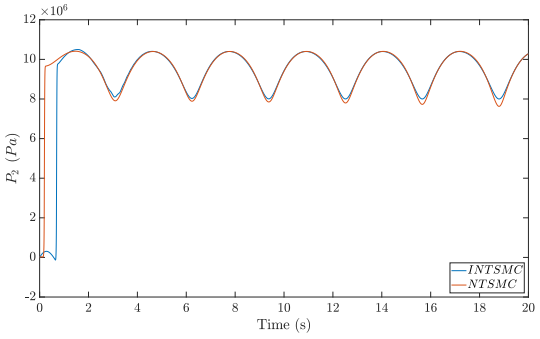

(b) Values of P_2

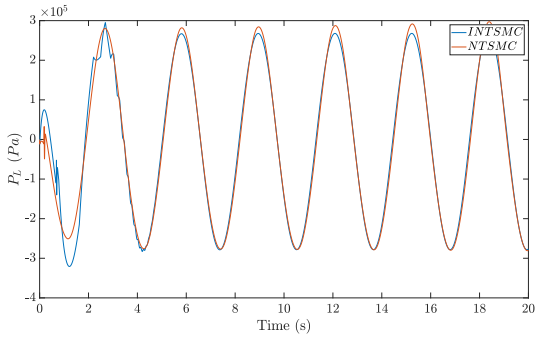

(c) Values of P_L

FIGURE 13. Values of the pressures of different part of the hydraulic circuit.

shown in Fig. 7 demonstrate that the controller obtained good performance and the states of the system reached the origin in a finite time. The proposed method is compared with an NTSMC introduced by [20]. The comparison between results demonstrates that the proposed approach converged more rapidly to zero. Clearly, the aim of the new method is to reach the position more rapidly and the results showed that the proposed controller performed better compared with the previous method. The RMSE for the controlled piston was employed as a feature for comparing the performance of the two controllers. The RMSE values were $RMSE_{INTSMC} = 0.08$ and $RMSE_{NTSMC} = 0.11$, thereby showing that the proposed controller obtained better performance than the NTSMC. The performances of the controllers using various parameters in the two methods are compared in Fig. 8. In order to confirm the feasibility of the method for actual implementation, the pressures in the different parts of the

hydraulic system are compared in Fig. 9. The pressure in the hydraulic systems was limited by a relief valve on the pump controller. Thus, the chamber pressures remained within an acceptable range under all conditions and independently of the controller.

To further analyze the controller, its capacity is investigated for tracking a desired trajectory, which was defined as follows.

$$\begin{aligned} x_d &= 0.15\sin(2t) + 0.3 \\ \dot{x}_d &= -0.3\cos(2t) \\ \ddot{x}_d &= -0.6\sin(2t) \end{aligned} \tag{30}$$

The results obtained using these functions as the desired trajectory of the hydraulic system are presented in Fig. 10. The proposed system is compared with the NTSM control approach presented by [20], where our proposed method performed better for the third-order system compared with the previous method. Both methods allowed the system states to track the desired trajectory but our proposed method reached the path and continued tracking it within a shorter time. To clearly illustrate the superior performance of the proposed method, the tracking errors with both methods are compared in Fig. 11. These results indicate that the tracking error was lower with the INTSMC method than the NTSMC method. The RMSE values for the tracking error using both methods are presented in Table 6. The development of the control signal and the sliding surface are also important factors that needed to be considered when evaluating the performance of the proposed controller, and the results for the control signal value and the sliding surface are presented in Fig. 12. The results in terms of the pressures on different sides of the cylinder and the load pressure are presented in Fig. 13.

IV. CONCLUSION

In this study, a new SMC method for nonlinear systems was proposed. An integral non-singular terminal surface was defined, and the proposed method was introduced for second-order systems. After considering the stability criteria, the new INTSMC controller was developed and expanded to nth-order systems. The stability of the controller was demonstrated and proven using Lyapunov theory by representing a global sliding surface for nth-order nonlinear systems. The application of an integral surface allows the system states to converge to the equivalent point more rapidly than the conventional non-singular terminal SMC. In addition, the proposed controller is not affected by the singularity phenomena found in previously introduced terminal SMC methods. The INTSMC method also performs well in the presence of external disturbances and uncertainties. The superior performance of the proposed controller was demonstrated based on its application to a 2-DoF robot manipulator as an example of a second-order system and to a third-order hydraulic system as an example of an nth-order system.

Owing to the superior performance of the INTSMC compared with conventional sliding mode controllers and its capacity to handle model uncertainties, it is planned to apply this controller to an experimental servo-hydraulic system setup in the Laboratory of Intelligent Machines at Lappeenranta University of Technology in future research. The overall model of this system is quite similar to the hydraulic model introduced in the present study, but small changes will be required.

REFERENCES

[1] T. Yang, N. Sun, H. Chen, and Y. Fang, "Neural network-based adaptive antiswing control of an underactuated ship-mounted crane with roll motions and input dead zones," *IEEE Trans. Neural Netw. Learn. Syst.*, to be published.

[2] N. Sun, D. Liang, Y. Wu, Y. Chen, Y. Qin, and Y. Fang, "Adaptive control for pneumatic artificial muscle systems with parametric uncertainties and unidirectional input constraints," *IEEE Trans. Ind. Informat.*, to be published.

[3] J.-J. E. Slotine and W. Li, *Applied Nonlinear Control*, vol. 199. Englewood Cliffs, NJ, USA: Prentice-Hall, 1991.

[4] Y. Yin, J. Liu, J. A. Sánchez, L. Wu, S. Vazquez, J. I. Leon, and L. G. Franquelo, "Observer-based adaptive sliding mode control of npc converters: An RBF neural network approach," *IEEE Trans. Power Electron.*, vol. 34, no. 4, pp. 3831–3841, Apr. 2018.

[5] U. K. Kalla, B. Singh, S. S. Murthy, C. Jain, and K. Kant, "Adaptive sliding mode control of standalone single-phase microgrid using hydro, wind, and solar PV array-based generation," *IEEE Trans. Smart Grid*, vol. 9, no. 6, pp. 6806–6814, Nov. 2018.

[6] M. Mohadeszadeh and H. Delavari, "Synchronization of fractional-order hyper-chaotic systems based on a new adaptive sliding mode control," *Int. J. Dyn Control*, vol. 5, no. 1, pp. 124–134, Mar. 2017.

[7] T. Elmokadema, M. Zribia, and K. Youcef-Toumi, "Terminal sliding mode control for the trajectory tracking of underactuated autonomous underwater vehicles," *Ocean Eng.*, vol. 129, pp. 613–625, Jan. 2017.

[8] S. Mobayen, "Adaptive global terminal sliding mode control scheme with improved dynamic surface for uncertain nonlinear systems," *Int. J. Control, Autom. Syst.*, vol. 16, no. 4, pp. 1692–1700, Aug. 2018.

[9] R. M. Asl, Y. Shabbouei Hagh, and H. Handroos, "Adaptive extended kalman filter designing based on non-singular fast terminal sliding mode control for robotic manipulators," in *Proc. IEEE Int. Conf. Mechatronics Autom. (ICMA)*, Aug. 2017, pp. 1670–1675.

[10] Y. Tang, "Terminal sliding mode control for rigid robots," *Automatica*, vol. 34, no. 1, pp. 51–56, 1998.

[11] L. Qiao and W. Zhang, "Adaptive non-singular integral terminal sliding mode tracking control for autonomous underwater vehicles," *IET Control Theory Appl.*, vol. 11, no. 8, pp. 1293–1306, Feb. 2017.

[12] R. M. Asl, E. Pourabdollah, and M. Salmani, "Optimal fractional order PID for a robotic manipulator using colliding bodies design," *Soft Comput.*, vol. 22, no. 14, pp. 4647–4659, Jul. 2018.

[13] R. M. Asl, A. Mahdoudi, E. Pourabdollah, and G. Klan ar, "Combined PID and LQR controller using optimized fuzzy rules," *Soft Comput.*, vol. 23, no. 13, pp. 5143–5155, Jul. 2019.

[14] P. Ouyang, J. Acob, and V. Pano, "PD with sliding mode control for trajectory tracking of robotic system," *Robot. Comput. Integr. Manuf.*, vol. 30, no. 2, pp. 189–200, 2014.

[15] C. Wang, L. Quan, S. Zhang, H. Meng, and Y. Lan, "Reduced-order model based active disturbance rejection control of hydraulic servo system with singular value perturbation theory," *ISA Trans.*, vol. 67, pp. 455–465, Mar. 2017.

[16] Y. Shabbouei Hagh, R. M. Asl, and V. Cocquempot, "A hybrid robust fault tolerant control based on adaptive joint unscented Kalman filter," *ISA Trans.*, vol. 66, pp. 262–274, Jan. 2017.

[17] R. Mohammadi Asl, Y. Shabbouei Hagh, and R. Palm, "Robust control by adaptive non-singular terminal sliding mode," *Eng. Appl. Artif. Intell.*, vol. 59, pp. 205–217, Mar. 2017.

[18] L. Zhang, L. Liu, Z. Wang, and Y. Xia, "Continuous finite-time control for uncertain robot manipulators with integral sliding mode," *IET Control Theory Appl.*, vol. 12, no. 11, pp. 1621–1627, Jul. 2018.

[19] H. Zhou, L. Lao, Y. Chen, and H. Yang, "Discrete-time sliding mode control with an input filter for an electro-hydraulic actuator," *IET Control Theory Appl.*, vol. 11, no. 9, pp. 1333–1340, Jun. 2017.

[20] Y. Feng, X. Yu, and Z. Man, "Non-singular terminal sliding mode control of rigid manipulators," *Automatica*, vol. 38, no. 12, pp. 2159–2167, 2002.
[21] H. Yousefi, H. Handroos, and J. K. Mattila, "Application of fuzzy gain-scheduling in position control of a servo hydraulic system with a flexible load," *Int. J. Fluid Power*, vol. 8, no. 2, pp. 25–35, 2007.
[22] M. Jelali and A. Kroll, *Hydraulic Servo-Systems: Modelling, Identification, and Control*. Berlin, Germany: Springer, 2012.
[23] H. Yousefi, H. Handroos, and A. Soleymani, "Application of differential evolution in system identification of a servo-hydraulic system with a flexible load," *Mechatronics*, vol. 18, no. 9, pp. 513–528, Nov. 2008.
[24] C. Guan and S. Pan, "Adaptive sliding mode control of electro-hydraulic system with nonlinear unknown parameters," *Control Eng. Pract.*, vol. 16, no. 11, pp. 1275–1284, 2008.
[25] Y. Qian, G. Ou, A. Maghareh, and S. J. Dyke, "Parametric identification of a servo-hydraulic actuator for real-time hybrid simulation," *Mech. Syst. Signal Process.*, vol. 48, nos. 1–2, pp. 260–273, Oct. 2014.

REZA MOHAMMADI ASL received the B.Sc. and M.Sc. degrees in electrical engineering, control systems from the University of Tabriz, Tabriz, Iran, in 2013 and 2015, respectively. He is currently a Junior Researcher with LUT University, Finland. His current research interests include nonlinear control, artificial intelligence, robotics, and hydraulic systems.

YASHAR SHABBOUEI HAGH received the M.Sc. degree in control engineering from the University of Tabriz, Iran, in 2016. He is currently a Junior Researcher with the Laboratory of Intelligent Machine, Department of Mechanical Engineering, LUT University, Finland. His research interests are focused on fault detection and diagnosis systems, fault tolerant controls, sliding mode controller, nonlinear Kalman filtering, and robotic manipulators. He is currently working on servo-hydraulic systems.

RAINER PALM received the Dr. Ing. degree from the Humboldt-University Berlin, Germany, in 1981, the Dr. sc. techn. degree (habilitation) from the Academy of Sciences, Germany, in 1989, and the Dipl.Ing. degree from the Technical University of Dresden, Germany, in 1975. He has been an Adjunct Professor and also a Guest Lecturer with the Department of Technology (AASS), University Örebro, since 2004. He was a Principal Research Scientist with Siemens Research and Development, Munich, Germany (1991–2004), the Research and Development with the Institute of Automatic Control, Berlin, Germany (1971–1981), and a Researcher with the Academy of Sciences, Berlin, Germany (1981–1991). He has authored or coauthored, edited or co-edited 20 books or chapters in books, and has authored/coauthored numerous articles in journals and conference proceedings. He is the author or coauthor of 14 patents. His research interests include automatic control, fuzzy control, system modeling, robotics, and mobile robots. He was the Spokesman of the Fuzzy Group, German Informatic Society (1994–2002). He was an Associate Editor of the IEEE TRANSACTIONS ON FUZZY SYSTEMS (1994-2004), and is an Associate Editor of the *Information Sciences*, since 2014.

HEIKKI HANDROOS received the M.Sc. (Eng.) and D.Sc. (Tech.) degrees from the Tampere University of Technology, in 1985 and 1991, respectively. He has been a Full Professor with the Lappeenranta University of Technology, since 1993. He has published about 300 scientific journal and conference papers. His research interests range from mechatronics and control to robotics. He is a member of the ASME and IEEE.